Article

Probing Helix Formation in Unsolvated Peptides

Gary A. Breaux, and Martin F. Jarrold

J. Am. Chem. Soc., **2003**, 125 (35), 10740-10747• DOI: 10.1021/ja0300362 • Publication Date (Web): 09 August 2003

J|A|C|S
ARTICLES
Published on Web 08/09/2003

Probing Helix Formation in Unsolvated Peptides

Gary A. Breaux and Martin F. Jarrold*

Contribution from the Chemistry Department, Indiana University, 800 East Kirkwood Avenue, Bloomington, Indiana 47405-7102

Received January 17, 2003; E-mail: mfj@indiana.edu

Abstract: Ion mobility measurements have been used to examine helix formation in unsolvated glycine-based peptides containing three alanine residues. Nine sequence isomers of Ac-[12G3A]K+H^+ were studied (Ac = acetyl, G = glycine, A = alanine, and K = lysine). The amount of helix present for each peptide was examined using two metrics, and it is strongly dependent on the proximity and the location of the alanine residues. Peptides with three adjacent alanines have the highest helix abundances, and those with well-separated alanines have the lowest. The helix abundances for most of the peptides can be fit reasonably well using a modified Lifson−Roig theory. However, Lifson−Roig theory fails to account for several key features of the experimental results. The most likely explanation for the correlation between helix abundances and the number of adjacent alanines is that neighboring alanines promote helix nucleation.

Introduction

Soon after the α-helix was first proposed by Pauling, Corey, and Branson in the early 1950s,[1] helix−coil transitions were observed for polypeptides in solution,[2] and statistical mechanical models were developed to explain these transitions. The original models of Zimm and Bragg[3] and Lifson and Roig[4] now form the basis for most modern helix−coil theories.[5] The basic idea behind these models is that there is a nucleation step that is associated with fixing a few residues into a helical configuration so that the first helix hydrogen bond can be made and then a propagation phase where residues add onto the end of the growing helix, each one making a new helix hydrogen bond.

The Zimm−Bragg and Lifson−Roig models approach the problem from different directions: the Zimm−Bragg model focuses on hydrogen bond formation, while Lifson−Roig focuses on residue conformations. Both models employ two parameters: a helix nucleation parameter that accounts for the entropy cost of fixing the first few residues into a helical conformation, and a helix propagation parameter that accounts for the free energy change of adding helical residues at the ends of an existing helix. The relationship between the two sets of parameters has been discussed by Qian and Schellman.[6]

The more recent helix−coil models are usually extensions of the Zimm−Bragg and Lifson−Roig models, but include refinements to improve agreement between theory and experiment such as the incorporation of 3−10 helices and end-capping effects.[7−11] The AGADIR model of MuZoz and Serrano[12,13] is a Lifson−Roig-based model that incorporates empirically many of the interactions that influence helix formation, including side chain interactions, electrostatics and helix dipole effects, N- and C-terminal preferences, and capping motifs. While the more refined models are better at reproducing the experimental results, the helix−coil parameters remain similar to those determined using the original theories.

The local environment experienced by a particular residue can influence helix formation through a complex array of interactions and steric effects. It has been known for some time that certain residues occur in nature with greater frequency in specific locations within helical domains.[14] One way of probing these context effects is through systematic permutations of the sequence. For example, Baldwin and collaborators found a decrease in the amount of helix present in an alanine-based peptide as a single glycine was moved closer to the center of the sequence.[15] Related studies have been performed to address the preference for particular residues near the N- and C-termini of short peptides.[16−19]

An aspect of helix formation that is difficult to address is the role of the solvent. One approach to this problem is to examine helix formation in solution and in a vacuum and to attribute the differences to the effects of the solvent.[20] Studies

(1) Pauling, L.; Corey, R. B.; Branson, H. R. *Proc. Natl. Acad. Sci. U.S.A.* **1951**, *37*, 205−211.
(2) Doty, P.; Yang, J. T. *J. Am. Chem. Soc.* **1956**, *78*, 498−500.
(3) Zimm, B. H.; Bragg, J. K. *J. Chem. Phys.* **1959**, *31*, 526−535.
(4) Lifson, S.; Roig, A. *J. Chem. Phys.* **1960**, *34*, 1963−1974.
(5) Doig, A. J. *Recent Advances in Helix-Coil Theory* (to be published).
(6) Qian, H.; Schellman, J. A. *J. Phys. Chem.* **1992**, *96*, 3987−3994.
(7) Doig, A. J.; Chakrabartty, A.; Klinger, T. M.; Baldwin, R. L. *Biochemistry* **1994**, *33*, 3396−3403.
(8) Rohl, C. A.; Chakrabartty, A.; Baldwin, R. L. *Protein Sci.* **1996**, *5*, 2623−2637.
(9) Stapley, J. S.; Rohl, C. A.; Doig, A. J. *Protein Sci.* **1995**, *4*, 2383−2391.
(10) Sheinerman, F. B.; Brooks, C. L. *J. Am. Chem. Soc.* **1995**, *117*, 10098−10103.
(11) Rohl, C. A.; Doig, A. J. *Protein Sci.* **1996**, *5*, 1687−1696.
(12) MuZoz, V.; Serrano, L. *Nat. Struct. Biol.* **1994**, *1*, 399−409.
(13) Lacroix, E.; Viguera, A. R.; Serrano, L. *J. Mol. Biol.* **1998**, *284*, 173−191.
(14) Richardson, J. S.; Richardson, D. C. *Science* **1988**, *240*, 1648−1652.
(15) Chakrabartty, A.; Schellman, J. A.; Baldwin, R. L. *Nature* **1991**, *351*, 586−588.
(16) Chakrabartty, A.; Doig, A. J.; Baldwin, R. L. *Proc. Natl. Acad. Sci. U.S.A.* **1993**, *90*, 11332−11336.
(17) Doig, A. J.; Baldwin, R. L. *Protein Sci.* **1995**, *4*, 1325−1336.
(18) Cochran, D. A. E.; Penel, S.; Doig, A. J. *Protein Sci.* **2001**, *10*, 463−470.
(19) Cochran, D. A. E.; Doig, A. J. *Protein Sci.* **2001**, *10*, 1305−1311.
(20) Jarrold, M. F. *Annu. Rev. Phys. Chem.* **2000**, *51*, 179−207.

10.1021/ja0300362 CCC: $25.00

of the conformations of unsolvated peptides and proteins have been made possible by the development of soft ionization methods.[21,22] In this work we use ion mobility mass spectrometry to examine the conformations of unsolvated peptides generated by electrospray. The mobility of an ion in an inert buffer gas depends on the average collision cross section. Ions with open conformations have more collisions with the buffer gas and travel more slowly than ions with compact conformations.[23−25] In previous work, it has been shown that this approach can be used to distinguish between helical and nonhelical conformations of unsolvated peptides.[26−31] In particular, Hartings et al. recently used this method to study helix formation in Ac-$A_4G_7A_4$+H^+ and Ac-$(AG)_7A$+H^+ peptides.[32]

One advantage of studying unsolvated peptides is that solubility is not an important issue. It is virtually impossible to study the highly hydrophobic Ac-$A_4G_7A_4$+H^+ and Ac-$(AG)_7A$+H^+ peptides mentioned above in aqueous solution. The recent studies have demonstrated that there are significant differences between the helix-forming tendencies of the different amino acids in aqueous solution and in the gas phase. In the gas phase, even glycine-rich peptides such as Ac-$A_4G_7A_4$+H^+ may show a significant helical component.

In this paper we describe a study of helix formation in a series of glycine-based peptides containing three alanines. Ion mobility measurements are used to provide two metrics of helix formation: (1) at low temperature the equilibrium between helical and nonhelical (globular) conformations is quenched and the amount of helix can be determined from the areas of the peaks due to the helical and globular conformations; and (2) at high temperatures, where interconversion between helical and globular conformations is rapid on the experimental time scale, the position of the measured peak relative to those expected for the helix and globule is used as a measure of the average amount of helix present. The results of these two measures of the percent helix appear to be closely correlated. Peptides with three neighboring alanine residues have the highest helical content, while those with separated alanine residues have the lowest. The results are compared to the predictions of a modified Lifson−Roig model,[7] which reproduces the main features of the helix abundances of the different peptides.

Methods and Materials

The peptides studied here were synthesized using *FastMoc* chemistry on an Applied Biosystems 433A peptide synthesizer. In *FastMoc*, the amino acids are activated with HBTU (2-(1*H*-benzotriazol-1-yl) 1,1,3,3-tetramethyluronium hexaflurophosphate). The peptides were cleaved from the HMP resin (4-hydroxymethyl-phenoxy-methyl-copolystyrene−1% divinyl benzene resin) using 5 mL of a 95% trifluoroacetic acid and 5% water v/v mixture. The glass-filtered supernatant was added to 45 mL of ethyl ether, and the peptide precipitate was collected and lyophilized. Solutions of 1−2 mg of the peptide in 1 mL of TFA and 0.01 mL of water were electrosprayed. All the peptides studied here have their N-termini acetylated and their C-termini unblocked.

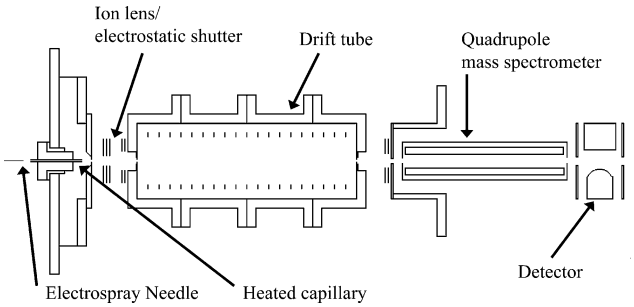

Figure 1. Schematic diagram of the electrospray ion mobility mass spectrometer used to study the conformations of unsolvated peptides.

Measurements were performed using a home-built, temperature-variable, electrospray ion-mobility mass spectrometer shown schematically in Figure 1 and fully described in a previous paper. Briefly, the peptide ions are electrosprayed and enter a differentially pumped region (∼0.25 mbar) through a heated capillary (330−400 K). The heated capillary aids in the desolvation process and reduces the abundance of multimers. The ions are then introduced into the main chamber of the apparatus, where a set of electrostatic lenses focuses them into the drift tube. The ions enter the drift tube with an injection energy of 200−600 eV. This energy is required to overcome the buffer gas flow out of the drift tube. Collisions with the buffer gas as they enter the drift tube cause a transient heating of the ions, but once the ions' kinetic energy is thermalized, their internal degrees of freedom are rapidly equilibrated to the buffer gas temperature.

The drift tube is 30.5 cm long, filled with 2.5−5.0 mbar of helium buffer gas, and maintained at temperatures ranging from 100 to 400 K with a precision of ±1 K. The drift tube is lined with a series of guard rings to ensure a uniform electric field along its length. The drift voltage was 280−480 V. Under these conditions ions undergo millions of collisions while traveling through the drift tube. After the ions exit the drift tube, they are focused into the last chamber of the apparatus, which contains a quadrupole mass spectrometer. After passing through the quadrupole, the ions are detected with an off-axis collision dynode and two stacked microchannel plates. The drift times (the amount of time it takes for the ions to travel across the drift tube) are determined using an electrostatic shutter to permit 100 μs packets of ions to enter the drift tube. The signals at the detector are then recorded using a multichannel scalar which is synchronized with the electrostatic shutter. The drift times can be easily converted into average collision cross sections.[33]

Results

Figure 2 shows drift time distributions (DTD) recorded for Ac-K$(G_4A)_3$+H^+, Ac-$(G_4A)_3$K+H^+, Ac-$G_8A_2G_4AK$+H^+, Ac-$G_{12}A_3K$+H^+, Ac-$A_3G_{12}K$+H^+, and Ac-$G_6A_3G_6K$+H^+ (Ac = acetyl, G = glycine, A = alanine, and K = lysine) at a low drift tube temperature (213 K) where interconversion between the helical and nonhelical conformation is slow compared to the experimental time scale. The peaks in the drift time distributions are assigned by comparing their cross sections to average collision cross sections calculated for conformations derived from molecular dynamics (MD) simulations. On this basis, the peaks at around 8.2 ms are assigned to helices, while those at around 7.0 ms are due to globules. The MD simulations

(21) Fenn, J. B.; Mann, M.; Meng, C. K.; Wong, S. F.; Whitehouse, C. M. *Science* **1989**, *246*, 64−71.
(22) Hillenkamp, F.; Karas, M.; Beavis, R. C.; Chait, B. T. *Anal. Chem.* **1991**, *63*, A1193−A1202.
(23) Hagen, D. F. *Anal. Chem.* **1979**, *51*, 870−874.
(24) Von Helden, G.; Hsu, M.-T.; Kemper, P. R.; Bowers, M. T. *J. Chem. Phys.* **1991**, *95*, 3835−3837.
(25) Clemmer, D. E.; Jarrold, M. F. *J. Mass Spectrom.* **1997**, *32*, 577−592.
(26) Hudgins, R. R.; Ratner, M. A.; Jarrold, M. F. *J. Am. Chem. Soc.* **1998**, *120*, 12974−12975.
(27) Hudgins, R. R.; Jarrold, M. F. *J. Am. Chem. Soc.* **1999**, *121*, 3494−3501.
(28) Hudgins, R. R.; Jarrold, M. F. *J. Phys. Chem. B* **2000**, *104*, 2154−2158.
(29) Kinnear, B. S.; Jarrold, M. F. *J. Am. Chem. Soc.* **2000**, *122*, 9234−9256.
(30) Kaleta, D. T.; Jarrold, M. F. *J. Phys. Chem. B* **2001**, *105*, 4436−4440.
(31) Kinnear, B. S.; Hartings, M. R.; Jarrold, M. F. *J. Am. Chem. Soc.* **2001** *123*, 5660−5667.
(32) Hartings, M. R.; Kinnear, B. S.; Jarrold, M. F. *J. Am. Chem. Soc.* (in press).
(33) Mason, E. A.; McDaniel, E. W. *Transport Properties of Ions in Gases*; Wiley: New York, 1988.

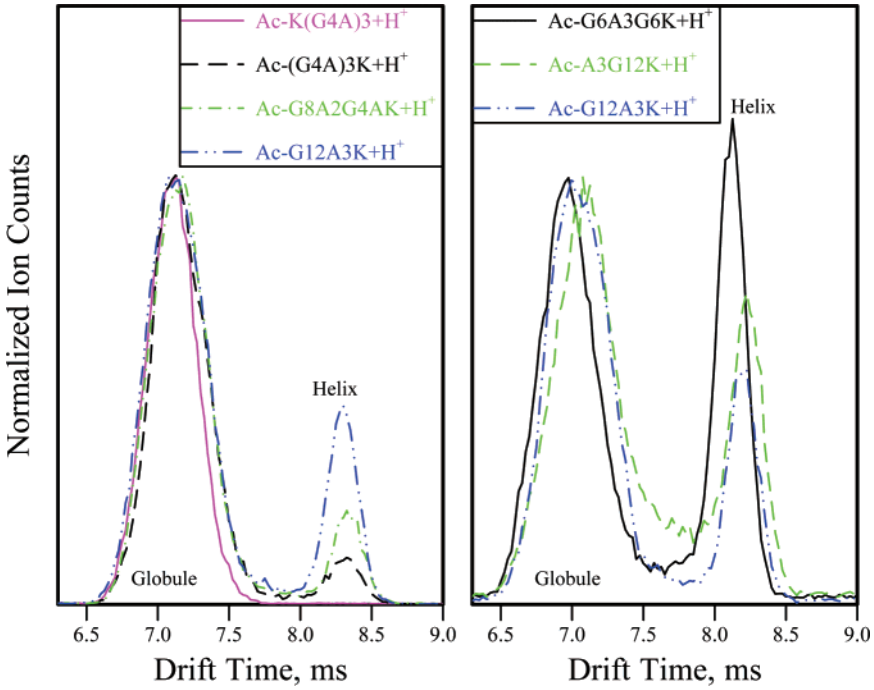

Figure 2. Drift time distributions recorded for Ac-K$(G_4A)_3$+H^+, Ac-$(G_4A)_3$K+H^+, Ac-$G_8A_2G_4AK$+H^+, Ac-$G_{12}A_3$K+H^+, Ac-A_3G_{12}K+H^+, and Ac-$G_6A_3G_6$K+H^+ at a low temperature (213 K), where interconversion between the helical and nonhelical conformation is slow compared to the experimental time scale. The distributions on the left illustrate the effect of adjacent alanines on the abundance of the helix, while the distributions on the right show the effect of moving an AAA group to different locations in the peptide (the N-terminus, the center, and the C-terminus).

were performed using the MACSIMUS suite of programs,[34] using the CHARMM 21.3 parameter set and a dielectric constant of 1.0. We assume that the peptides are protonated at the lysine side chain (see below for more discussion of this issue). Average collision cross sections were calculated using the empirically corrected exact hard spheres scattering model[35] from 50 snapshots taken from the last 35 ps of the simulations. If the structures sampled in the MD simulations match those present in the experiments, the measured and calculated cross sections are expected to agree to within 2%. Examples of helical and globular conformations taken from the MD simulations for Ac-A_3G_{12}K+H^+ are shown in Figure 3. Note that the C-terminus end of the helix in Figure 3 is a partial π-helix. This is a common feature of helical conformations derived from the MD simulations for these peptides and apparently results because it allows more backbone CO groups to interact with the charged lysine side chain. The globules are compact random-looking three-dimensional structures; these compact conformations are preferred in the gas phase to the random coil geometries generally believed to be present in solution, because of the absence of solvent.

The relative abundances of the helical and globular conformations evident in Figure 2 are not representative of the relative abundances in solution (the peptides studied here are not expected to be significantly helical in solution). The ions are collisionally heated and then rapidly cooled as they are injected into the drift tube, and the resulting distribution of conformations represents the helix−globule equilibrium for the unsolvated peptides at the temperature where interconversion is quenched as the ions are cooled. This temperature is unknown, though it

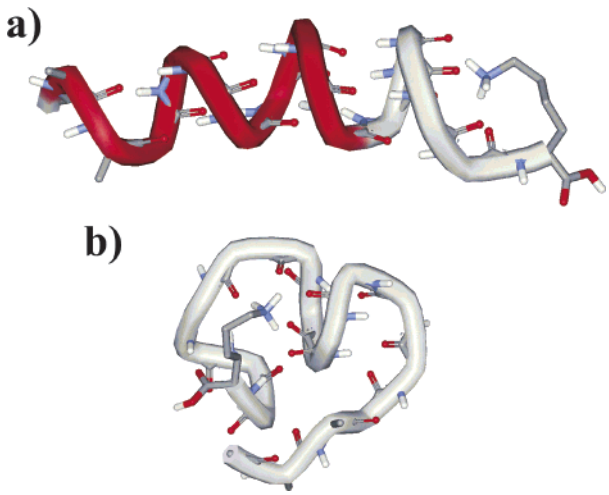

Figure 3. Representative helix (a) and globule (b) conformations from the molecular dynamics simulations for the Ac-A_3G_{12}K+H^+ peptide.

is evidently larger than the drift tube temperature used to record the data in Figure 2 (213 K).

Note in Figure 2 that Ac-K$(G_4A)_3$+H^+ does not form a helix (there is no peak for this peptide at around 8.2 ms), while Ac-$(G_4A)_3$K+H^+ does form a helix. This dramatic difference in the conformational preference is attributed to the lysine carrying the charge.[26,27] When the charge is at the C-terminus, as in Ac-$(G_4A)_3$K+H^+, the interaction between the charge and the helix macro-dipole is favorable. When the charge is at the N-terminus as in Ac-K$(G_4A)_3$+H^+, the interaction is unfavorable and no helix is observed. The lysine side chain is the most basic site for these peptides in aqueous solution. But in the gas phase, protonation at the amide CO groups is expected to become competitive, so the location of the protonation site in the gas phase is not as clear-cut as in solution. Some studies of the

(34) Kolafa, J. http://www.icpf.cas.cz/jiri/macsimus/default.htm.
(35) Kinnear, B. S.; Kaleta, D. T.; Kohtani, M.; Hudgins, R. R.; Jarrold, M. F. *J. Am. Chem. Soc.* **2000**, *122*, 9243−9256.

Table 1. Percent Helix Values Determined from the Drift Time Distributions Measured at 213 and 391 K[a]

		percent helix			
peptide sequence	type[b]	experiment at "213 K"	Doig–Lifson–Roig fit to "213 K"	experiment at 391 K	Doig–Lifson–Roig fit to 391 K
Ac-GGGGGG**AAA**GGGGGGK	AAA	36	38	32	33
Ac-**AAA**GGGGGGGGGGGK	AAA	26	24	38	37
Ac-GGGGGGGGGGG**AAA**K	AAA	21	14	27	17
Ac-GGGGGGGG**AA**GGGG**A**K	AA	10	13	18	17
Ac-GGGGGGGGG**A**GGG**AA**K	AA	10	13	14	17
Ac-GGG**A**GGGGG**A**GGGG**A**K	A	6	4	13	16
Ac-GGGG**A**GGGG**A**GGGG**A**K	A	6	5	14	16
Ac-GGGGG**A**GGG**A**GGGG**A**K	A	7	7	13	17
Ac-GGGGGGGGG**A**G**A**GG**A**K	A	4	14	12	17
Ac-**AAA**GGGGGGGGGGGK	AAA	26	24		
Ac-**AAA**GGGGGGGGGGGGGK	AAA	26	23		
Ac-**AAA**GGGGGGGGGGGGGGGK	AAA	20	20		
Ac-GGGGGGGGGGGGGGGK		1	10^{-6}		

[a] The percent helix values deduced from modified Lifson−Roig theory are shown for comparison. Note that the real temperature associated with the 213 K measurements (the temperature where the population distribution is frozen-in) is unknown. [b] AAA indicates three adjacent alanines, AA indicates two adjacent alanines, and A indicates no adjacent alanines.

dissociation of peptide ions in the gas phase have been interpreted as indicating that the protons are mobile.[36,37] However, this mobility is driven by the excess internal energy present in the dissociation studies. At close to room temperature (and below) if one site is significantly more basic than the others, the proton is expected to be localized. In what follows we assume that the lysine side chain is the protonation site (as inferred from the experimental results).

To determine the amount of helix present in the DTDs measured at 213 K, the helix peak was fit with a Gaussian, then the percent helix was calculated by dividing the area of the Gaussian by the area of the entire drift time distribution. Note that this calculation assumes that the area under the Gaussian is attributed entirely to a fully formed helix (i.e., the conformation is 100% helical). We are not able to distinguish between a conformation that is almost entirely helical (95%) and a conformation that is 100% helical, because of the limitations of our experimental method, and this could serve as a potential source of error with the derived values. However, the width of the helical peak indicates that it represents a single conformation (or a narrow range of conformations with almost identical cross sections), and the measured cross section is in good agreement with that calculated for fully helical conformations from MD simulations. Note that the peak assigned to the globular conformation is broader than expected for a single structure, indicating that a series of compact random-looking conformations contribute to this feature.

Table 1 shows the percent helix values derived from the analysis described above. From these results, and from Figure 2, two trends are evident. The first trend is a strong correlation between the amount of helix and the number of immediately adjacent alanines. The AAA peptides (peptides with three neighboring alanines) have a higher percent helix (21−36%) than the AA peptides (10%), which in turn have a higher percent helix than the A peptides (4−7%). The second trend evident in Table 1 and Figure 2 is that the percent helix decreases when alanines are moved away from the center of the peptide. The percent helix decreases the most with a movement of the alanines from the center toward the C-terminus. The AAA peptides at 213 K are obvious examples of this position trend, with Ac-$G_6A_3G_6K+H^+$ having 36% helix (alanines at the center), Ac-$A_3G_{12}K+H^+$ at 26% (alanines at the N-terminus), and Ac-$G_{12}A_3K+H^+$ at 21% (alanines at the C-terminus). The Ac-$G_9AGAG_2AK+H^+$ peptide, which has the lowest percent helix value of the Ac-[12G3A]$K+H^+$ sequence isomers tested (4% at 213 K), has a combination of the adjacent and position trends discussed above, having no adjacent alanines and all of the alanines shifted toward the C-terminus.

Further studies were conducted on some additional peptides to examine the role of glycine in helix formation. Ac-$A_3G_{13}K$ and Ac-$A_3G_{15}K$ were synthesized to compare with Ac-$A_3G_{12}K$. As can be seen from Table 1, the addition of the extra glycine(s) reduces the percent helix: Ac-$A_3G_{12}K+H^+$ has 26% helix, Ac-$A_3G_{13}K+H^+$ has 26% helix, and Ac-$A_3G_{15}K+H^+$ has 20% helix. We also synthesized the polyglycine analogue of the 16-residue peptides (Ac-$G_{15}K$). Even though glycine is a strong helix breaker in the aqueous phase,[38] a small but measurable helix peak was observed for Ac-$G_{15}K+H^+$. The percent helix in the 213 K drift time distributions is around 1%.

Figure 4 shows a plot of the drift time distributions for the Ac-$G_{12}A_3K+H^+$ peptide recorded as a function of drift tube temperature. To be able to directly compare the drift time distributions recorded at different temperatures, the drift time axis was converted to a cross section axis, and then the cross section scale was adjusted to 300 K values. This was done by fitting a function to the cross sections for the Ac-$K(G_4A)_3+H^+$ peptide (which is believed to have a nonhelical conformation over the entire temperature range examined) and using this function to scale the cross sections. The unscaled cross sections systematically decrease as the temperature is raised because the long-range interactions between the ion and the buffer gas become less important and the collisions become harder and ride further up the repulsive wall as the temperature rises.

In Figure 4, two peaks are resolved for Ac-$G_{12}A_3K+H^+$ at 213 K which are assigned to helical (∼265 Å^2) and globular (∼225 Å^2) conformations. As the temperature is raised, the helical peak decreases in intensity, and the intensity in the bridge region between the two peaks increases. This indicates that the helix is converting into the globule as the ions travel through the drift tube. If an ion starts traveling across the drift tube in

(36) Dongre, A. R.; Jones, J. L.; Somogyi, Á.; Wysocki, V. *J. Am. Chem. Soc.* **1996**, *118*, 8365−8374.
(37) Burlet, O.; Orkiszewski, R. S.; Ballard, K. D.; Gaskell, S. J. *Rapid Commun. Mass Spectrom.* **1992**, *6*, 658−662.
(38) Chakrabartty, A.; Baldwin, R. L. *Adv. Protein Chem.* **1995**, *46*, 141−176.

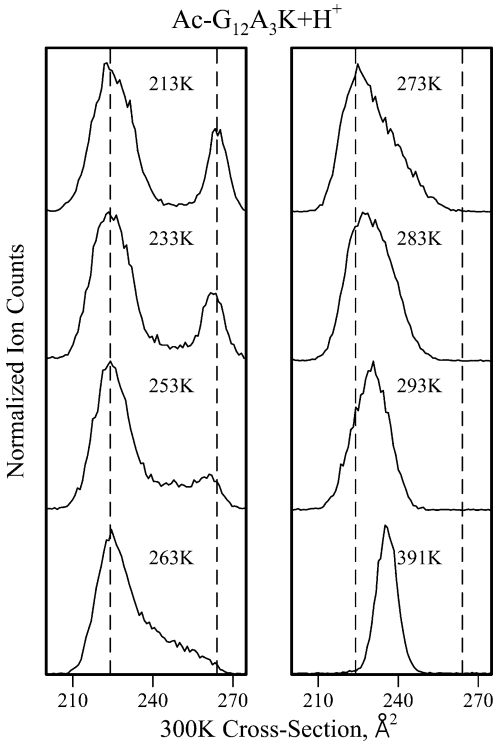

Figure 4. Plot of $AcG_{12}A_3K+H^+$ drift time distributions vs drift tube temperature. To be able to compare drift time distributions measured at different temperatures, the drift time scale has been converted to a cross section scale, and then the cross sections have been scaled to 300 K as described in the text.

a helical conformation and converts into a globule halfway across, its drift time will be halfway between that of the helix and the globule, and thus fall in the bridge region between the peaks (so intensity between the helix and globule peaks does not necessarily indicate the existence of species with long-lived structures intermediate between the helix and globule). At 273 K, the helix peak has essentially gone and there is a broad peak centered close to the position of the globule at low temperature. At this temperature we appear to be in a kinetic domain where the helix can overcome the activation barrier to convert into the globule, but the globule does not so readily return to the helical state. The rate of the helix→globule transition is expected to be larger than the rate of the globule→helix transition because at slightly higher temperatures the equilibrium favors the globule.

As the temperature is raised further, the peak narrows, and at 391 K there is a single narrow peak that lies between the positions expected for the helix and globule. When interconversion between two states is rapid compared to the time scale of the drift time measurement, there is a single narrow peak in the drift time distribution and its position reflects the amount of time spent in each state. In the present case, the fraction of the time spent in the helical state provides a measure of the equilibrium constant between the helix and globule. To obtain the fraction of the time spent as a helix at 391 K, the cross section for the measured peak was compared to cross sections expected for the helix and globule. The expected cross section for the helix was obtained by scaling the cross section calculated for an ideal α-helix at 300−391 K. This was done by scaling the function that fit the cross sections for the $Ac\text{-}K(G_4A)_3+H^+$ peptide (see above) so that it went through the calculated cross section for an ideal α-helix at 300 K. The scaled line also went through the points assigned to the helix at low temperature, which validates this approach. For the expected cross section for the globule at 391 K, we used the measured cross section for the $Ac\text{-}K(G_4A)_3+H^+$ peptide. The fraction of time spent as a helix (percent helix) is then given by the difference between the cross section of the ideal helix and the experimental value at 391 K, divided by the difference between the ideal helix and the ideal globule at 391 K.

Table 1 shows the percent helix values determined at 391 K. The strong correlation between the amount of helix and the number of immediately adjacent alanines is evident. The AAA peptides have a higher percent helix (from 27 to 38%) than the AA peptides (14−18%), which in turn have a higher percent helix than the A peptides (12−14%). The percent helix also decreases as the alanines are moved from the center of the peptide. Thus the $Ac\text{-}G_8A_2G_4AK+H^+$ peptide has a larger percent helix than $Ac\text{-}G_9AG_3A_2K+H^+$ (18% versus 14%). The percent helix for the $Ac\text{-}A_3G_{12}K+H^+$ peptide appears to be anomalous in comparison with the trends observed in the 213 K DTDs (see Table 1). We will discuss this issue further below.

Discussion

There is good overall agreement between the two measurements of the percent helix shown in Table 1. For the low-temperature measurements, where the helix−globule equilibrium is quenched, the amount of helix can be reasonably accurately defined. However, it is not possible to assign a temperature to the equilibrium constant determined in this way because it is not known at what temperature the helix−globule equilibrium is quenched. At high temperature, where the helix and globule are in rapid equilibrium and the temperature can be defined, there is some concern about how accurately the position of the peaks reflects the amount of helix present. The uncertainty in the cross sections for the ideal helix and globule at 391 K means that the relative uncertainty is largest at the extremes (high and low percent helix).

The approach used to analyze the high-temperature data is only strictly valid for a two-state system where there is helix and globule, but not a significant abundance of partially helical states. The low-temperature DTDs which show peaks for helices and globules, but little between, are consistent with this all-or-nothing behavior. Previous kinetic studies of the helix→globule transition in the $Ac\text{-}(AGG)_5K+H^+$ peptide were also consistent with such a two-state interpretation. However, there remains the possibility that for the present peptides the peaks at 391 K are due to the formation of an intermediate structure (not fully helical or globular) that is perhaps stabilized by entropic factors, rather than being due to a rapid equilibrium between the helical and globular conformations. The close correspondence between the helical values deduced from the two metrics argues against this third structure interpretation but does not rule it out. There is also the possibility that partially helical structures could exist as long-lived intermediates at the higher temperatures where the helix and globule are actively interconverting. The presence of such long-lived intermediates would influence the experimental results, but their effect is probably small.

While there is a good correlation between the percent helix values determined using the two metrics, there are a few differences. Perhaps the most notable difference occurs for Ac-

$G_6A_3G_6K+H^+$ and Ac-$A_3G_{12}K+H^+$. The percent helix is greater for Ac-$G_6A_3G_6K+H^+$ than for Ac-$A_3G_{12}K+H^+$ in the 213 K DTDs, while the reverse is true for the values derived from the 391 K measurements. In the drift time distributions shown in Figure 2, the helix and globule peaks for the Ac-$G_6A_3G_6K+H^+$ peptide are at slightly lower cross sections than for the other peptides studied. Thus the cross sections used for the ideal helix and globule may be slightly too large for this peptide, and this would lead to an underestimate of the amount of helix present for the Ac-$G_6A_3G_6K+H^+$ peptide at 391 K.

To gain insight into the origin of the trends evident in the measured percent helix values for the different peptides, we have attempted to fit our results using a modified Lifson−Roig model that incorporates an adjustment to allow for contributions from the N- and C-terminus capping effects.[7] As described above, Lifson and Roig theory is a statistical mechanical model to describe helix formation. There is a nucleation step, which requires the fixing of three residues into an α-helical conformation, followed by a propagation phase (which can occur from both ends of the helix). Helix unfolding is the reverse of this process (within the framework of the model) and occurs by unraveling from the ends of the helical regions.

The modified Lifson−Roig model uses four parameters: the (temperature-independent) helix nucleation parameter (v), which is associated with the entropic cost of fixing a residue into the α-helical conformation without the benefit of a helix hydrogen bond; the (temperature-dependent) helix propagation parameter (w), which is related to the equilibrium constant for switching a residue between helical and nonhelical states; and the N-terminus capping parameter (n) and the C-terminus capping parameter (c), which account for end effects including helix anisotropy. The measured quantity, the percent helix, is given by

$$\theta_h = \frac{100}{N}\frac{\delta \ln Z}{\delta w} \tag{1}$$

where N is the number of helical hydrogen bonds formed and Z is the Lifson−Roig partition function. The matrix form of the modified Lifson−Roig[7] partition function is

$$Z = e\prod_{i=1}^{N} W_i e^+ \tag{2}$$

with

$$W_i = \begin{bmatrix} w_i & v_i & 0 & 0 \\ 0 & 0 & \sqrt{n_i c_i} & c \\ v & v & 0 & 0 \\ 0 & 0 & n & 1 \end{bmatrix} \qquad e^+ = \begin{bmatrix} 0 \\ 0 \\ 0 \\ 1 \end{bmatrix} \qquad e = [0 \;\; 0 \;\; 0 \;\; 1] \tag{3}$$

A complete discussion of the partition function and the percent helix is given in the review by Poland and Scheraga.[39]

The modified Lifson−Roig model was fit to both sets of percent helix values for the Ac-[12G3A]K+H^+ peptides. The calculations were done using a MathCAD solve block to find the best fit for a system of nine equations for θ_h, one for each Ac-[12G3A]K+H^+ peptide in Table 1. The helix nucleation (v) and propagation (w) parameters for alanine, glycine were allowed to adjust freely (there are no propagation or nucleation parameters for the residues at the ends of the peptide). The n parameter for the acetyl group and the c parameter for the lysine were also allowed to adjust freely. The n and c parameters for alanine and glycine were set to 1. By setting the n and c parameters for a particular residue to 1, the matrix collapses to the original Lifson−Roig form.

Table 2. Comparison of Helix−Coil Parameters (Zimm−Bragg notation) Deduced for Alanine and Glycine in Unsolvated Peptides (this work) to Those Determined in Aqueous Solution[a]

			aqueous solution	
helix–coil parameter	unsolvated, "213 K" (this work)	unsolvated, 391 K (this work)	host–guest, 293 K (Scheraga[40])	substitution, 273 K (Baldwin[41])
σ(glycine)	3.2×10^{-7}	2.7×10^{-10}	1.0×10^{-5}	0.0011
σ(alanine)	0.0039	8.1×10^{-5}	8.0×10^{-4}	0.0011
s(glycine)	0.684	1.108	0.59	0.046
s(alanine)	170.5	297.4	1.07	1.64
n(acetyl)	2.805	5.539	NA	8.94 (ref 7)
c(lysine)	0.241	0.561	NA	NA

[a] σ is the helix nucleation parameter, s is the helix propagation parameter, and n and c are the helix-capping parameters. Note that the real temperature associated with the 213 K measurements (the temperature where the population distribution is frozen-in) is unknown.

The helix nucleation and propagation parameters for alanine and glycine obtained from the fits are shown in Table 2. The parameters are listed in Zimm−Bragg notation. The conversion between Lifson−Roig and Zimm−Bragg parameters has been described by Qian and Schellman ($s = w/(v + 1)$ and $\sigma = v^2/(1 + v)^4$). We have also included in Table 2 the helix nucleation and propagation parameters determined for glycine and alanine in aqueous solution from the host−guest studies of Scheraga and collaborators[40] and the small peptide substitution studies of Baldwin and collaborators.[41] Perhaps the most notable difference between the gas phase and aqueous phase parameters is the large helix propagation parameter (s) for alanine in the unsolvated peptides. Such a large helix propagation parameter is necessary to describe the strong helix-forming tendencies observed in the gas phase. The value determined for the helix propagation parameter (s) for glycine indicates that glycine weakly destabilizes the formation of the helix. This is in agreement with the aqueous phase studies of Scheraga and coworkers.[40] The helix nucleation parameter (σ) for alanine is much greater than the σ parameter for glycine. This would indicate that helix nucleation predominately occurs with the alanines. The σ variable is expected to be temperature independent, but our values show a significant difference between the values obtained from the two data sets, though this could at least partly result from experimental differences and uncertainties. We have already discussed a reason the percent helix measured for the Ac-$G_6A_3G_6K+H^+$ peptide at 391 K may be underestimated. The value of the c parameter determined for lysine from both data sets is less than 1, which indicates that lysine is helix-destabilizing. This conflicts with the known helix-stabilizing effects of a charged lysine at the C-terminus.[26,27] The low value for the c parameter is necessary to account for the fact that the amount of helix is lower when the alanines are close to the C-terminus. The value for the n parameter for the

(39) Poland, D.; Scheraga, H. A. *Theory of Helix-Coil Transitions in Biopolymers*; Academic: New York, 1970.
(40) Wojcik, J.; Altmann, K. H.; Scheraga, H. A. *Biopolymers* **1990**, *30*, 121−134.
(41) Rohl, C. A.; Chakrabartty A.; Baldwin, R. L. *Protein Sci.* **1996**, *5*, 2623−2637.

acetyl group is greater than 1 to account for the increase in the probability of forming a helix when the alanines are near the N-terminus.

The percent helix values obtained from the Lifson−Roig model (using the nucleation and propagation parameters derived above) are shown in Table 1, where they can be compared with the measured values. The agreement between the measured and calculated percent helix values is quite good overall. The calculated trends are in better agreement with the percent helix values determined from the low-temperature measurements. For the Ac-$G_9AGAG_2AK+H^+$ peptide, the calculated value is significantly higher than the measured one in both data sets. In the Lifson−Roig calculations the percent helix for the Ac-G_9-$AGAGGAK+H^+$ peptide is very similar to that for Ac-G_9-$AGGGAAK+H^+$. Both peptides have the alanines grouped together near the C-terminus; an AGA unit in the first peptide substitutes for a GAA in the second. However, while the Ac-$G_9AGAG_2AK+H^+$ peptide looks like the other AA peptides in the Lifson−Roig calculations, it looks like the other A peptides in the experiments.

Both of the major trends evident in the experimental data (the effect of the number of adjacent alanines and their position in the peptide) are reproduced by the modified Lifson−Roig model (see Table 1). A higher helix abundance when the alanines are located near the center of the sequence results in the Lifson−Roig model because a greater number of helical states incorporate the central residues than the residues at the termini. If a helix nucleates in the center, it can propagate from both ends, while if a helix nucleates at one of the termini, it can propagate in only one direction. This trend can be offset in the modified Lifson−Roig model by the effects of the *n* and *c* capping parameters. Helix formation at the N-terminus is promoted by a large value for the *n* parameter for the acetyl group and diminished at the C-terminus by a small value for the *c* parameter. This is evident in the 391 K results, where Ac-$A_3G_{12}K+H^+$ has a greater percent helix than Ac-G_6-$A_3G_6K+H^+$.

The enhancement in the percent helix with the number of adjacent alanines might be thought to result from increased helix nucleation. Within the framework of the Lifson−Roig model it requires three residues to nucleate a helix, and since alanine has a larger helix nucleation parameter than glycine (see Table 2), a group of three alanines will have a higher probability for helix nucleation than a group of three glycines. To examine the role of helix nucleation in determining the calculated percent helix values, we set the nucleation parameters for alanine and glycine to their weighted average and re-ran the Lifson−Roig calculations. Changing the nucleation parameters had a major effect on the calculated values. We repeated the same experiment with the propagation parameters; this also produced drastic changes in the helical content. This indicates that both helix nucleation and propagation are important for the model's prediction of the high percent helix values for the AAA peptides. Having a high concentration of alanines close together provides the peptide with a localized region where residues have a high probability of being found in a helical state. By keeping this region helical the amount of helix is increased overall. This is a cooperative effect, where localizing the residues with a higher propensity to be helical leads to an overall increase in the percent helix. This explains why the calculated percent helix for the Ac-$G_9AGAG_2AK+H^+$ peptide is so large (compared with those for the other A peptides); this peptide has the alanines grouped together (though not adjacent).

The preceding discussion points to a significant difference between the predictions of the Lifson−Roig model and the experimental results for these peptides. In the Lifson−Roig model the peptides are partially helical: there is a distribution of percent helix values centered around the average. The percent helix value here really refers to the fraction of the peptide that is helical. In the experiments, the low-temperature results indicate that the peptides are either helical or globular. Here, the percent helix value refers to the fraction of the peptides that are helices. It is likely that this all-or-nothing behavior also occurs in the experiments at higher temperatures (where the helix and globule are freely interconverting). However, while our results favor this interpretation, they are inconclusive on this point. The all-or-nothing behavior may result from the helix-stabilizing effects of the charge. The presence of the helix in the unsolvated peptides is largely the result of a favorable interaction between the charge (which is believed to be located on the lysine side chain near the C-terminus) and the helix macro-dipole. If the lysine residue is moved to the N-terminus, the charge−dipole interactions become unfavorable and the helix is not observed. The strong helix-stabilizing interactions between the charge and the helix dipole may help to lock-in the helical conformation, so that once it is formed, it is difficult to disrupt.

In contrast to the predictions of the Lifson−Roig model, where peptides with the alanines grouped together (though not necessarily adjacent) have a high percent helix, the experimental results show a tighter correlation with the number of adjacent alanines. This difference is most clearly illustrated by the results for the Ac-$G_9AGAG_2AK+H^+$ peptide (see Table 1). It appears that the explanation provided by the Lifson−Roig model that a high percent helix results from a cooperative effect, where localizing the residues with a higher propensity to be helical leads to an overall increase in the percent helix, is not correct. The tighter correlation with the number of *adjacent* alanine residues indicates that neighboring alanines promote helix formation. Thus the most likely explanation for this behavior is that neighboring alanines promote helix nucleation by restricting the conformation space.

Conclusions

By combining the results of this study with those from previous studies it is now evident that there are three major factors influencing helix formation in unsolvated peptides. The first in the location of the charge.[26,27] A positive charge close to the C-terminus promotes helix formation by favorable interactions with the helix macro-dipole, while a positive charge at the N-terminus is helix destabilizing. A second factor controlling helix formation in the gas phase is the relative free energy of the nonhelical state, a compact globule. Previous work has shown that the helix-forming tendency of glycine, alanine, valine, and leucine reflects their ability to pack compact low-energy globular states. Thus valine with bulky side chains has a stronger tendency to form helices in the gas phase than alanine not because the helix is more favorable for valine but because the alternative (the globule) is less favorable.[42]

(42) Kinnear, B. S.; Jarrold, M. F. *J. Am. Chem. Soc.* **2001**, *123*, 7907−7908.

The results presented in this paper reveal that context is the third important factor controlling helix formation in unsolvated peptides. The location of three alanines within a glycine-based peptide was found to change the percent helix over a range of almost an order of magnitude. The dominant trend evident from the experimental data is that neighboring alanines promote helix formation. This effect appears to result from enhanced helix nucleation when the alanines are neighbors. While the experimental percent helix values could be fit by a modified form of Lifson−Roig theory incorporating N- and C-terminus capping, the parameters deduced from the fit were often quite different from their solution values. The modified Lifson−Roig theory fails to account for several key features of the experimental results including the apparent all-or-nothing character of helix formation and the helix-stabilizing effects of the C-terminus lysine. Some of these deficiencies may result from differences in the nonhelical state in the gas phase and solution. In solution (and in the statistical mechanical models) the transition is a helix−coil transition where the nonhelical state is a random coil, while in the gas phase the transition is a helix−globule transition. It may be beneficial to develop a statistical mechanical model for the helix−globule transition for the gas phase and other environments with a low dielectric constants.

Acknowledgment. We gratefully acknowledge the support of this work by the National Institutes of Health. We thank Jiri Kolafa for the use of his MACSIMUS programs.

JA0300362